International Journal of Advances in Engineering and Management (IJAEM)
Volume 4, Issue 1 Jan 2022, pp: 410-424 www.ijaem.net ISSN: 2395-5252

Modeling of Body Centered Cubic and Face Centered Cubic Crystallographic Lattice Structures for Instructional Purposes of Atomic Packing Factor Computation

John Akpan John and Ephraim Richard Afia

Submitted: 02-01-2022 Revised: 09-01-2022 Accepted: 12-01-2022

ABSTRACT
Modelling of BCC and FCC crystallographic lattice structures for instructional purposes of Atomic packing factor computation is aimed at demonstrating to students the authenticity of the subject through the creation of optical appreciation and an immersion into reality tailored towards enhancing students' comprehension of concept of these structures and providing a tangible grasp of the differences and similarities between these structures with regards to Atomic Packing Factor (APF) computation. The modelling of the structures began with the creation of AutoCAD drawing of the intended structures. The AutoCAD drawings are then interpreted in Standard Tessellation Language (STL) of additive manufacturing used in 3D printing and followed by slicing; a process that translates the 3D drawing into a form the 3D printer can understand and print. The half and quarter balls created by means of 3D printing are systemically glued together using adhesive to form two sets of BCC and FCC crystallographic structures for instructional purpose of APF computation. The APF for BCC and FCC computed gave a numerical value of 0.68 and 0.74 respectively. Findings from results also indicated that the speed of printing of the models is inversely proportional to the time of printing of the models while each infill percentage and speed of printing of the models is directly proportional to the total time of printing and total lines of printing of the models respectively.

Keywords: Crystallographic, Atomic Packing Factor, Computation.

I. INTRODUCTION

The demand of teaching-learning process in 21st century is a challenge to Educational Institution and requires rethinking the methods of teaching in order to gain pedagogical advantages (Jorge et al., 2015). This is very important in this rapidly changing setting especially when dealing with abstract concepts. Research has revealed that learning can be enhanced and abstract concepts easily understood when models are created for instructional purposes (Stephen et al., 2002) This method of learning will not only expand the student baseline knowledge regarding the subject under discussion but will also promote conception change and accelerate misconception repair (Krause, 2012).

To this end, the study of crystallography due to its abstract nature will be immaterial especially for germinating students and teachers of materials science, metallurgy and crystal chemistry, if the traditional two-dimensional (2D) concept in still adopted while teaching and learning the concept of crystal structures. Another challenge is the minute nature of these crystals that makes it a herculean task to be studied and observed with unaided human eye. It is therefore, against this backdrop, that this research work seeks to create models of the BCC and FCC crystallographic lattice structures for instructional purposes of APF computation. These models when produced, assembled and packaged in transparent boxes for instructional purpose will enable an immersion into reality tailored towards enhancing students understanding of the concept of these structures and therefore, providing them with an adequate optical appreciation of the structures with regards to APF computation.

II. MATERIALS AND METHODS

Materials properties selected for the purpose of accomplishing the creation of these models are ease of processing & surface finishing, strong bonding ability, physical strength, aesthetic and transparency.

Thus, the materials used for the production of the model are

International Journal of Advances in Engineering and Management (IJAEM)
Volume 4, Issue 1 Jan 2022, pp: 410-424 www.ijaem.net ISSN: 2395-5252

- Thermoplastic filament (Poly lactic acid) (PLA)
- Adhesive glue (super glue)
- Acrylic

Thermoplastic filament

Thermoplastics make up most of the types of filament used in deposition modeling. Filament made from thermoplastic material can be used in 3D printing to create many different colors, even transparent or glow in the dark

Adhesive Glue (Super Glue)

Adhesive also known as glue or paste (as shown in plate II) is a nonmetallic substance applied to one or both surfaces of two separate items that binds them together and resists their separation. It is a substance that binds the surface of each model together. Thus, for the models to be closely packed to portray its structure, super glue is applied.

Acrylic

Acrylic polymer is a group of polymers (plastics) noted for transparency and elasticity (as shown in Plate III) It is also a glassy thermoplastic used in molding or in coating the ball to show its aesthetics.

METHODS

The methods adopted for the production of these models is presented in the flow chart below

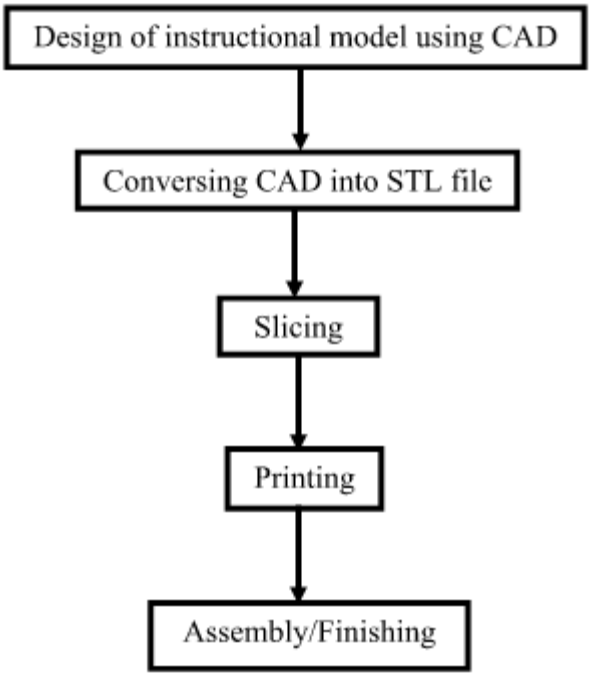

The methods adopted for this project are explained below:

- **Modeling:** Instructional models of Body Centered Cubic (BCC) and Face Centered Cube (FCC) for the computation of Atomic Packing Factor (APF) is designed using CAD software, otherwise known as 3D modeling software. In this, the software shapes the models to the required specifications to reduce errors, allowing verification in the design of the models prior to printing. At this point, the crystal structures are drawn, paying attention to the dimensions of the models for Body Centered Cubic (BCC) and Face Centered Cube (FCC). Figures 2.1 and 2.2 show the assembled CAD models for Body Centered Cubic (BCC) and Face Centered Cube (FCC) crystallographic lattice structures for the computation of Atomic Packing Factor (APF) respectively, while Figures 2.3 and 2.4 show the model that will be printed.

International Journal of Advances in Engineering and Management (IJAEM)
Volume 4, Issue 1 Jan 2022, pp: 410-424 www.ijaem.net ISSN: 2395-5252

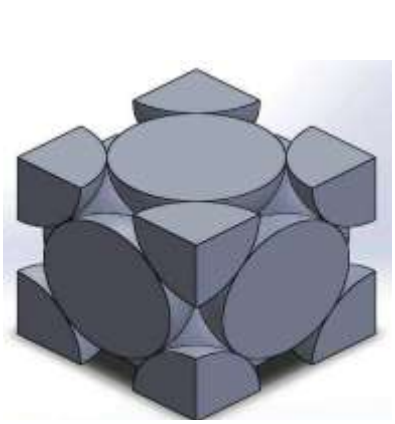

Figure 2.1: CAD Model for BCC Structure

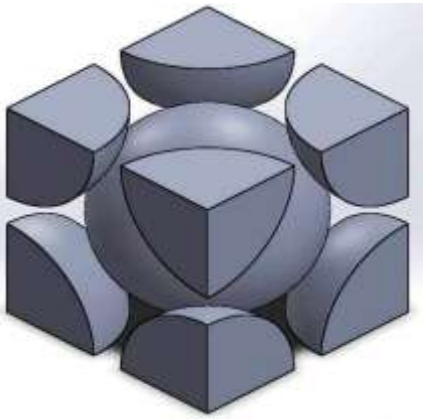

Figure 2.2: CAD Model for FCC structure

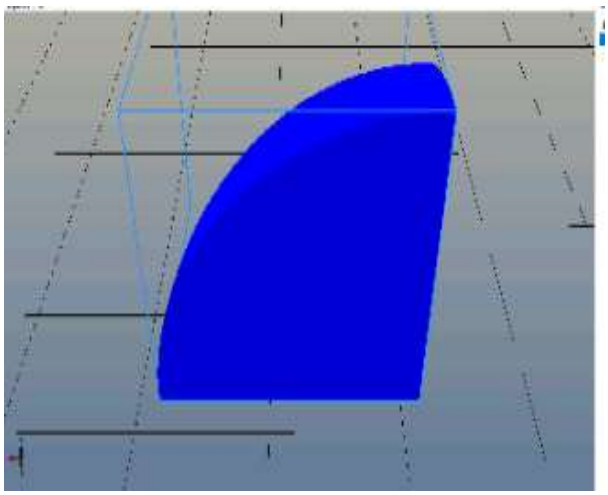

Figure 2.3: Quarter Ball

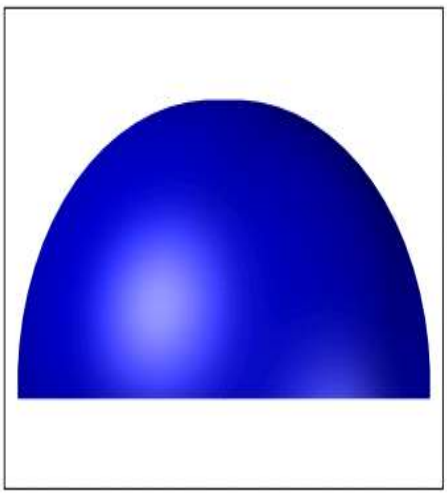

Figure 2.4: Half Ball

- **STL File**: The Standard Tessellation Language (Standard Triangle Language) file stores information about 3D models which in turn described the surface geometry of the 3D model without representing the color or texture of the model. In other words, the STL file examines the model for errors in surface mesh, self–intersections, etc. The concept called tessellation is the process of filling a surface with one or more geometric shapes such that there is no overlap.

- **Slicing**: The next method is slicing. At this stage, the CAD drawing for Body Centered Cubic (BCC) and Face Centered Cube (FCC) is sliced using slicing software which will translate the 3D drawing into a form that a 3D printer can understand and print. In other words, slicing turns digital 3D models into G-code (a generic name for a control language) that a 3D printer can understand, like layer slice and tooth path. Slicing software is necessary because the 3D printer could not translate CAD drawing by itself. Slicing software also creates a path for the 3D printer to follow before printing. These paths are instructions for geometry, what speed to print as to various points and what layer thickness to adopt. The CAD file is sliced into thin layers which is sent to the 3D printer. From there, the slicer sends codes in G-code format to the 3D printer. The slicing software file used is CuraEngine.

- **Printing**: After converting the CAD drawing into STL (Standard Tessellation Language) and slicing done, the next stage is the printing process. The type of 3D printer used is FDM (Fused Deposition Modeling). In this printer, a spool of thermoplastic filament is used and an extruder with a hot nozzle of about 200^{o}C which extruded the plastic through a cone shaped metal piece called a hot end into a small thin strand at the point of

International Journal of Advances in Engineering and Management (IJAEM)
Volume 4, Issue 1 Jan 2022, pp: 410-424 www.ijaem.net ISSN: 2395-5252

moving around the three-dimensional XYZ planes by dropping layer upon layer until the required shape of the model is formed. This process is repeated until all the models are formed.

- **Assembly**: The assembling of the models for Body Centered Cubic (BCC) and Face Centered Cube (FCC) crystallographic lattice structure for the computation of Atomic Packing Factor (APF) is done through the help of adhesive glue (Araldite). The models created by 3D printing are joined together as shown in Figure 2.1 and 2.2 for Body Centered Cubic (BCC) and Face Centered Cubic (FCC) respectively.

Computation of Atomic Packing Factor (APF) for BCC Crystal Structure.

- - (3.1)

To determine the atomic radius of BCC Structure, we extract the top plane of the BCC in the Plate I below.

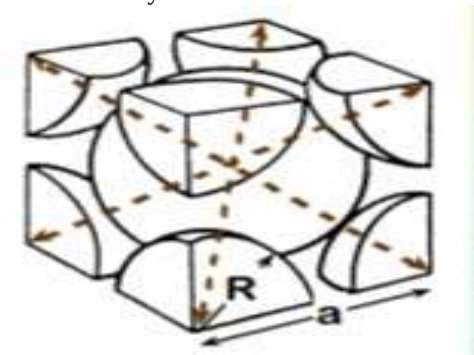

Plate I: BCC Crystal Structure

Source:(Adikwanduaba, 2005)

From Plate VIII, we have that

- - - - - (3.2)

- - - - - (3.3)

Taking square root of both sides, we have;

- - - - - - (3.4)

Using Pythagoras'sTheorem

- - - - - (3.5)

Recalling that , hence the new equation becomes

- - - - - (3.6)

- - - - - (3.7)

Making r, the subject of formulae, we have;

- - - - - (3.8)

Taking the root of both sides, we have;

- - - - - (3.9)

Therefore;

Recall that,

where,

- - (3.10)

Substituting, into (10), we have;

Computation of Atomic Packing Factor (APF) for FCC Crystal Structure.

- - (3.11)

- - - - - - (3.12)

International Journal of Advances in Engineering and Management (IJAEM)
Volume 4, Issue 1 Jan 2022, pp: 410-424 www.ijaem.net ISSN: 2395-5252

To determine the atomic radius of FCC Structure, we extract the top plane of the FCC in the Plate I1 below.

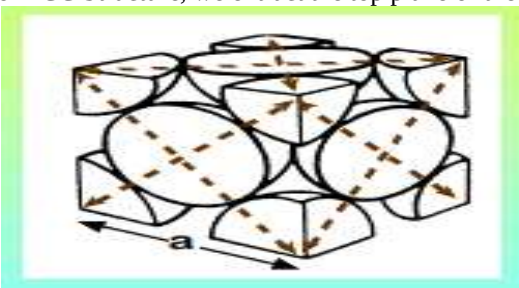

Plate II: FCC Crystal Structure

Source: (Adikwanduaba, 2005)

- - - - (3.13)
- - - (3.14)

Equating (3) and (4), we have;

Making r, the subject of formulae, we have;

Therefore;

- - - (3.15)

Volume of the unit cell

- - - (3.16)

Therefore;

- - - - - (3.17)

Substituting, into (7), we have

III. RESULTS

The results obtained from the printing process are outlined in Tables 3.1 – 3.9 and Figures 3.1 – 3.9.

Table 3.1: Results for Printing Speed and Time of Printing at 0% Infill

At 0% Infill (Half Balls)			
Printing Speed (Millimeter per Second)	**Printing Speed (Meter per Second)**	**Time of Printing (Seconds)**	**Time of Printing (Hours)**
40	**0.040**	**5048**	**1.402**
45	**0.045**	**5044**	**1.401**
50	**0.050**	**5032**	**1.398**
55	**0.055**	**5028**	**1.397**

International Journal of Advances in Engineering and Management (IJAEM)
Volume 4, Issue 1 Jan 2022, pp: 410-424 www.ijaem.net ISSN: 2395-5252

60	**0.060**	**5008**	**1.391**

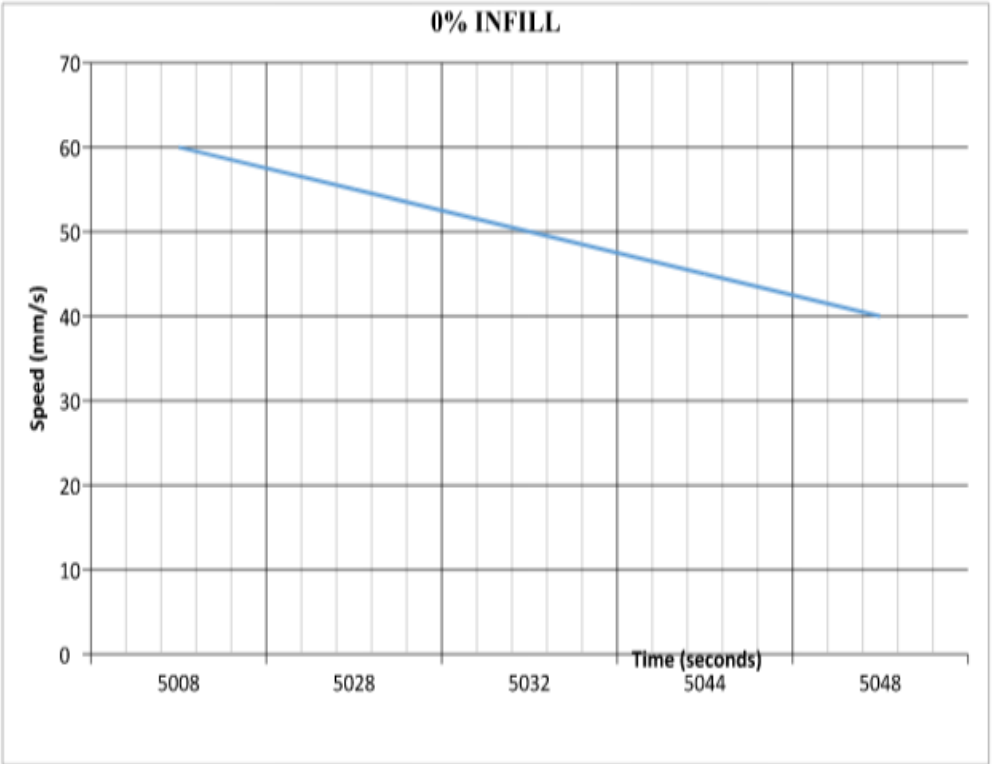

Figure 3.1: Graph of Printing Speed against Time of Printing at 0% Infill

Table 3.2: Results for Printing Speed and Time of Printing at 20% Infill

At 20% Infill (Half Balls)			
Printing Speed (Millimeter per second)	**Printing Speed (Meter per second)**	**Time of Printing (Seconds)**	**Time of Printing (Hours**
40	**0.040**	**5048**	**1.474**
45	**0.045**	**5044**	**1.392**
50	**0.050**	**5032**	**1.388**
55	**0.055**	**5028**	**1.387**
60	**0.060**	**5008**	**1.385**

International Journal of Advances in Engineering and Management (IJAEM)
Volume 4, Issue 1 Jan 2022, pp: 410-424 www.ijaem.net ISSN: 2395-5252

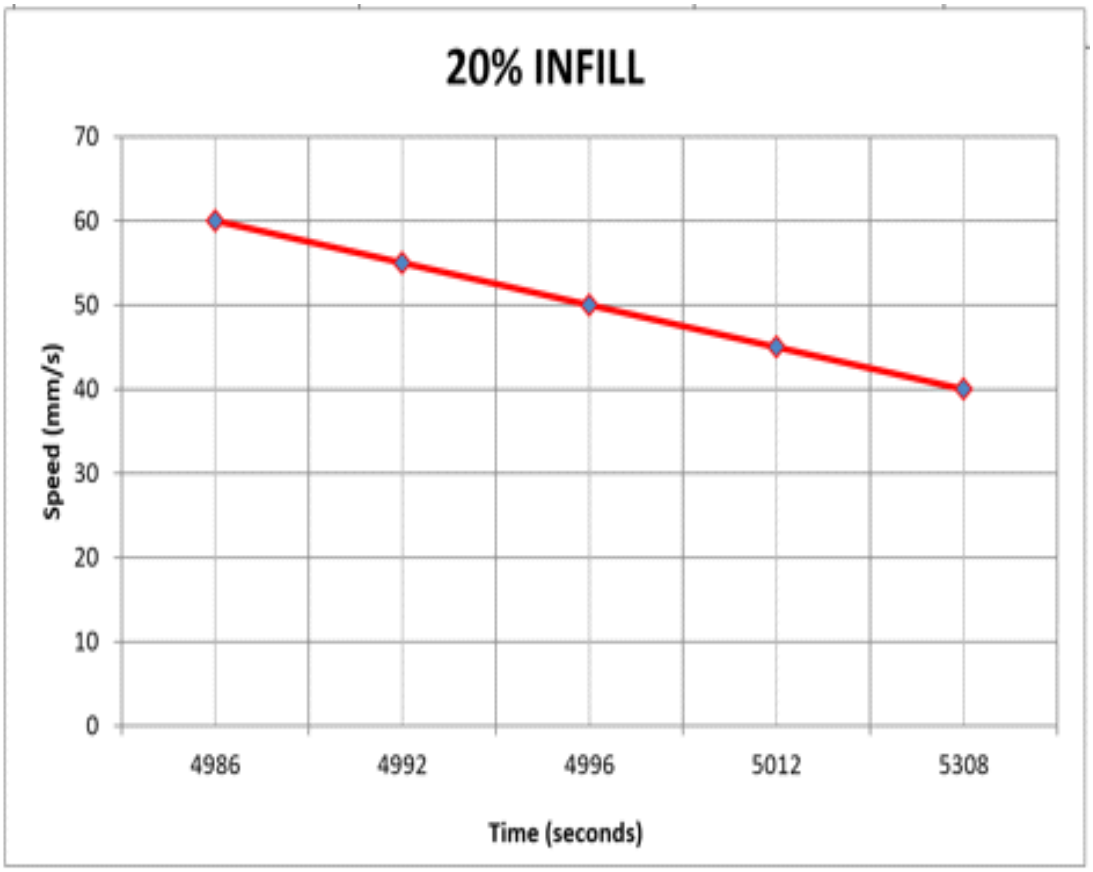

Figure 3.2: Graph of Printing Speed against Time of Printing at 20% Infill

Table 3.3: Results for Printing Speed and Time of Printing at 40% Infill

At 40% Infill (Half Balls)			
Printing Speed (Millimeter per second)	**Printing Speed (Meter per second)**	**Time of Printing (Seconds)**	**Time of Printing (Hours**
40	**0.040**	**5672**	**1.576**
45	**0.045**	**5280**	**1.467**
50	**0.050**	**5228**	**1.452**
55	**0.055**	**4982**	**1.384**
60	**0.060**	**4944**	**1.373**

International Journal of Advances in Engineering and Management (IJAEM)
Volume 4, Issue 1 Jan 2022, pp: 410-424 www.ijaem.net ISSN: 2395-5252

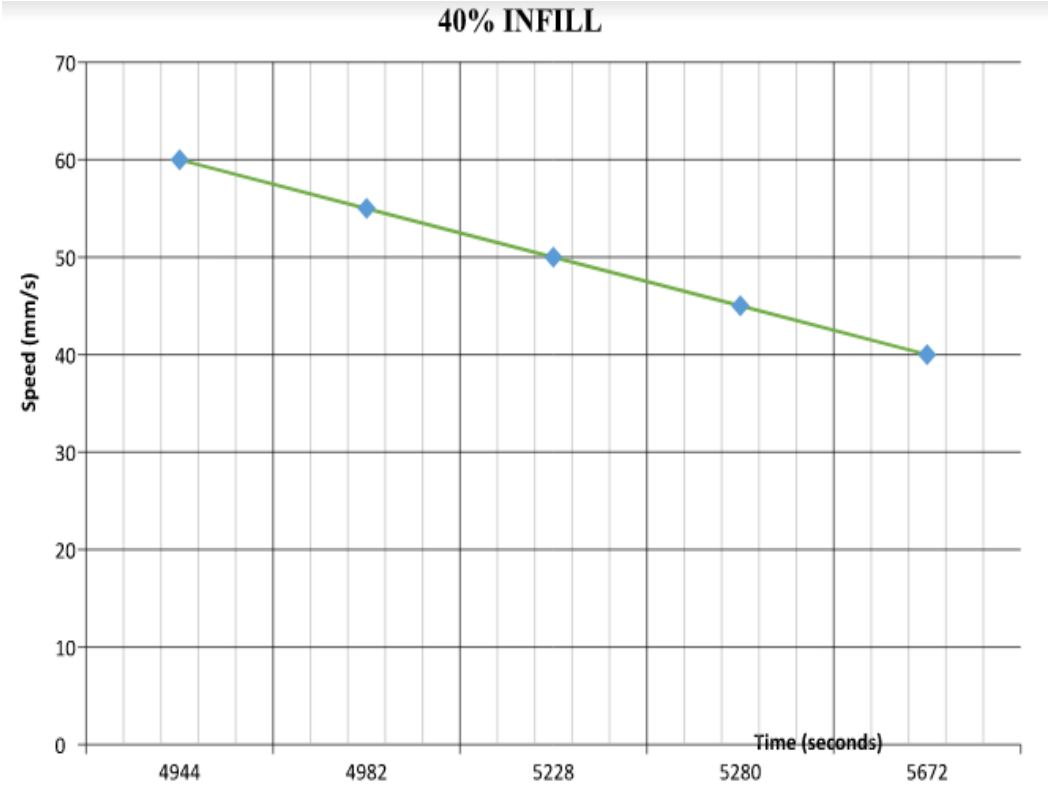

Figure 3.3: Graph of Printing Speed against Time of Printing at 40% Infill

Table 3.4: Results for Printing Speed and Time of Printing at 60% Infill

At 60% Infill (Half Balls)			
Printing Speed (Millimeter per second)	**Printing Speed (Meter per second)**	**Time of Printing (Seconds)**	**Time of Printing (Hours)**
40	**0.040**	**6216**	**1.727**
45	**0.045**	**5760**	**1.6**
50	**0.050**	**5460**	**1.517**
55	**0.055**	**5224**	**1.451**
60	**0.060**	**5164**	**1.434**

International Journal of Advances in Engineering and Management (IJAEM)
Volume 4, Issue 1 Jan 2022, pp: 410-424 www.ijaem.net ISSN: 2395-5252

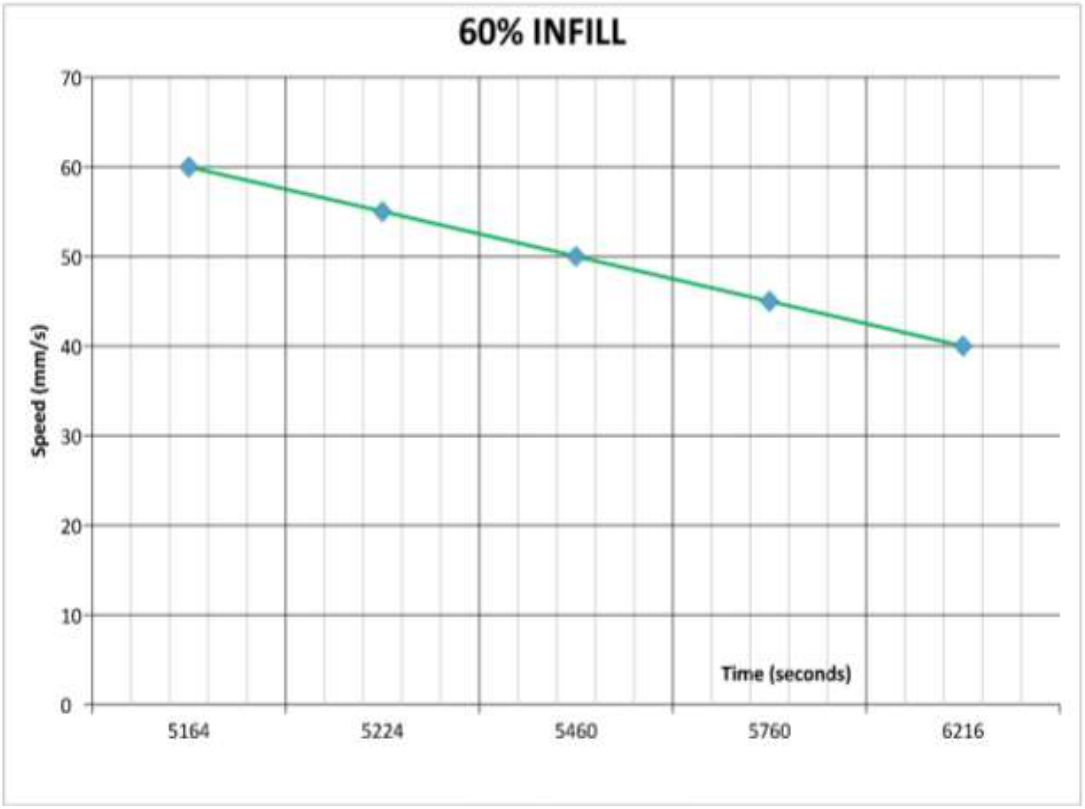

Figure 3.4: Graph of Printing Speed against Time of Printing at 60% Infill

Table 3.5: Results for Printing Speed and Time of Printing at 80% Infill

At 80% Infill (Half Balls)			
Printing Speed (Millimeter per second)	**Printing Speed (Meter per second)**	**Time of Printing (Seconds)**	**Time of Printing (Hours)**
40	**0.040**	**6732**	**1.87**
45	**0.045**	**6228**	**1.73**
50	**0.050**	**6028**	**1.674**
55	**0.055**	**5668**	**1.574**
60	**0.060**	**5588**	**1.552**

International Journal of Advances in Engineering and Management (IJAEM)
Volume 4, Issue 1 Jan 2022, pp: 410-424 www.ijaem.net ISSN: 2395-5252

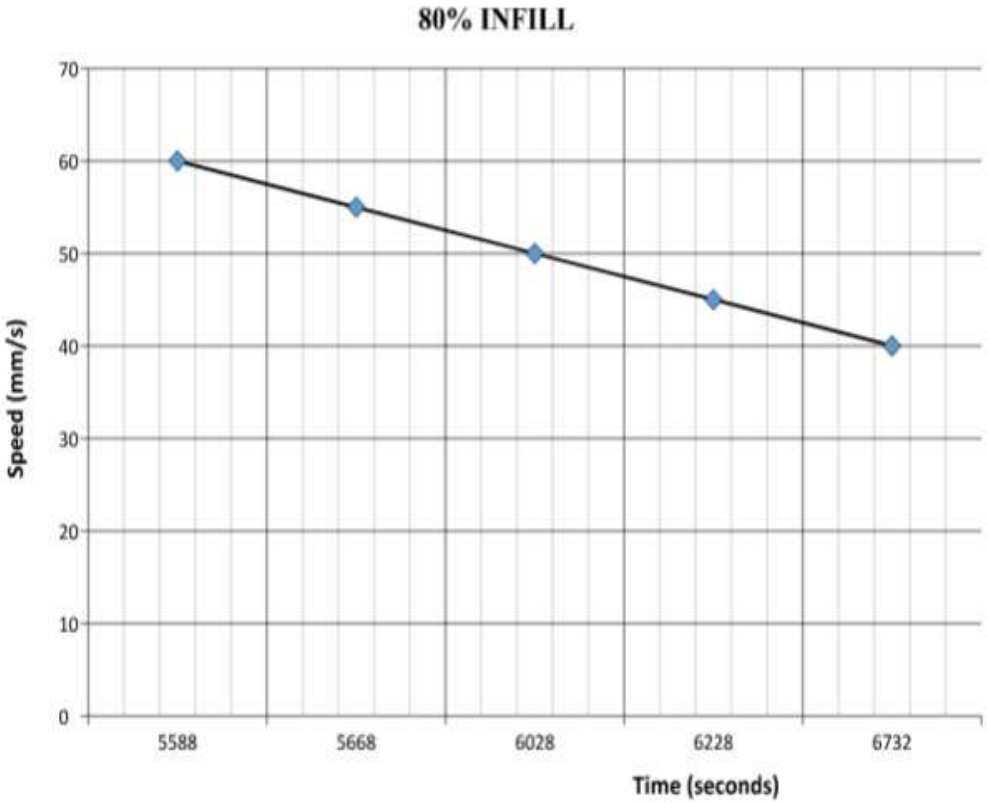

Figure 3.5: Graph of Printing Speed against Time of Printing at 80% Infill

Table 3.6: Results for Printing Speed and Time of Printing at 100% Infill

At 100% Infill (Half Balls)			
Printing Speed (Millimeter per second)	**Printing Speed (Meter per second)**	**Time of Printing (Seconds)**	**Time of Printing (Hours)**
40	**0.040**	**7192**	**1.998**
45	**0.045**	**6656**	**1.849**
50	**0.050**	**6260**	**1.739**
55	**0.055**	**5920**	**1.644**
60	**0.060**	**5672**	**1.576**

International Journal of Advances in Engineering and Management (IJAEM)
Volume 4, Issue 1 Jan 2022, pp: 410-424 www.ijaem.net ISSN: 2395-5252

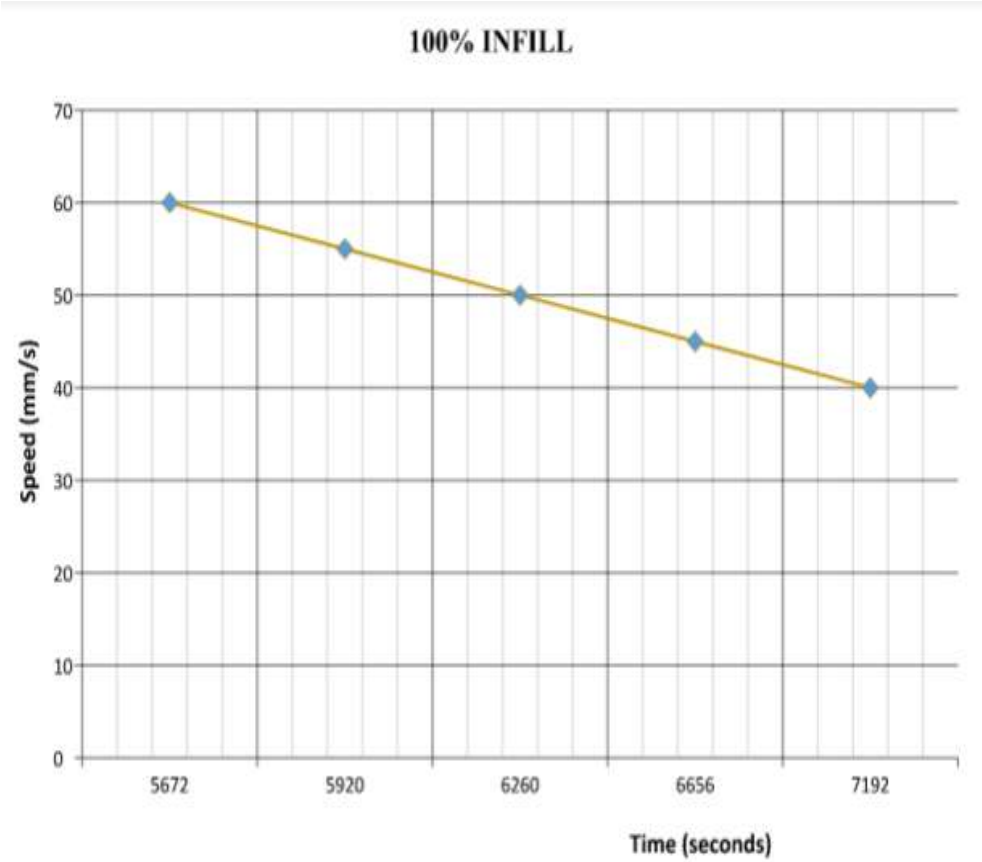

Figure 3.6: Graph of Printing Speed against Time of Printing at 100% Infill

Table 3.7: Relationship between Infill % and Total Time of Printing of the Half Balls.

Percentage Infill (%)	Total Time of Printing (Seconds)	Total Time of Printing (Hours)
0	**25080**	**6.967**
20	**25204**	**7.001**
40	**26104**	**7.251**
60	**27816**	**7.727**
80	**30164**	**8.379**
100	**31588**	**8.774**

International Journal of Advances in Engineering and Management (IJAEM)
Volume 4, Issue 1 Jan 2022, pp: 410-424 www.ijaem.net ISSN: 2395-5252

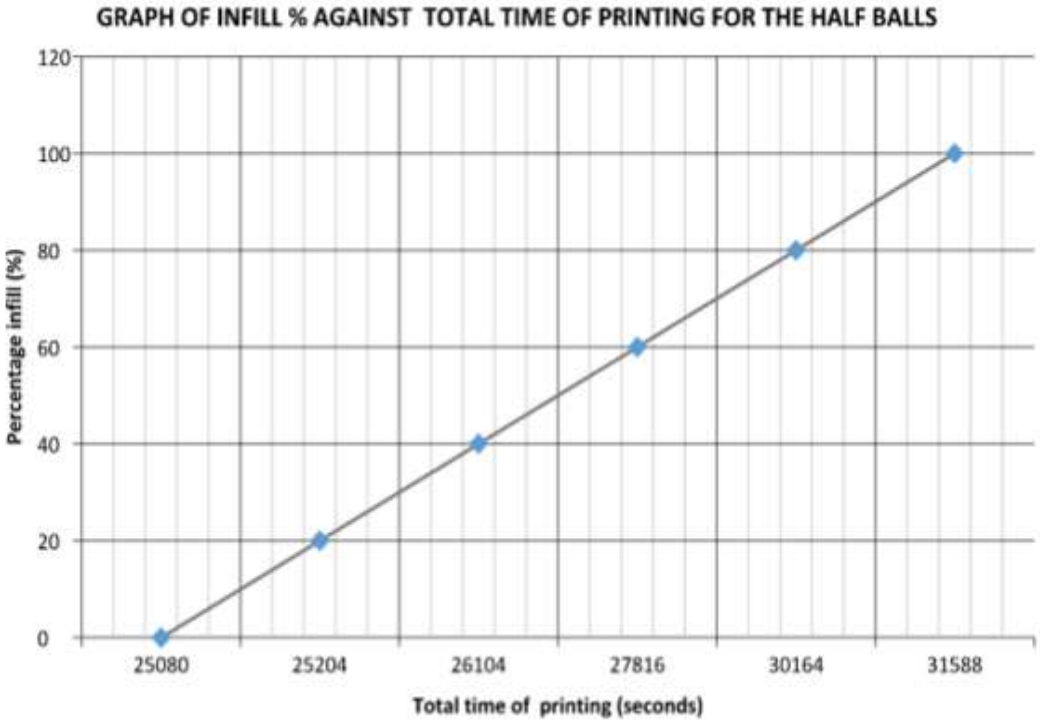

Figure 3.7: Relationship between Infill % and Total Time of Printing of the Half Balls

Table 3.8: Results for printing speed and total lines at 0% infill

At 0% infill (Quarter Balls)	
Printing speed (Millimeter per Second)	**Total lines**
40	**11093**
45	**11095**
50	**11096**
55	**11126**
60	**11142**

International Journal of Advances in Engineering and Management (IJAEM)
Volume 4, Issue 1 Jan 2022, pp: 410-424 www.ijaem.net ISSN: 2395-5252

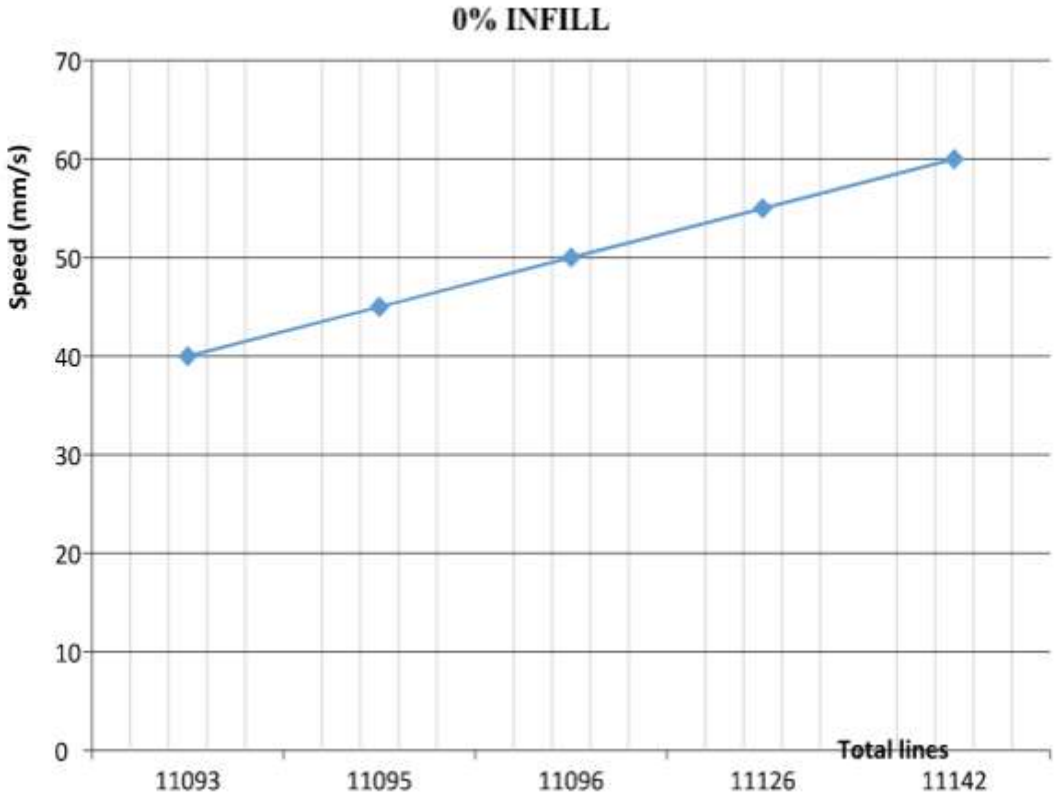

Figure 3.8: Graph of printing speed against total lines of printing for quarter balls.

Table 3.9: Results for printing speed and total lines at 100% infill

At 100% infill (Quarter Balls)	
Printing speed (millimeter per second)	**Total lines**
40	16309
45	16310
50	16312
55	16314
60	16317

International Journal of Advances in Engineering and Management (IJAEM)
Volume 4, Issue 1 Jan 2022, pp: 410-424 www.ijaem.net ISSN: 2395-5252

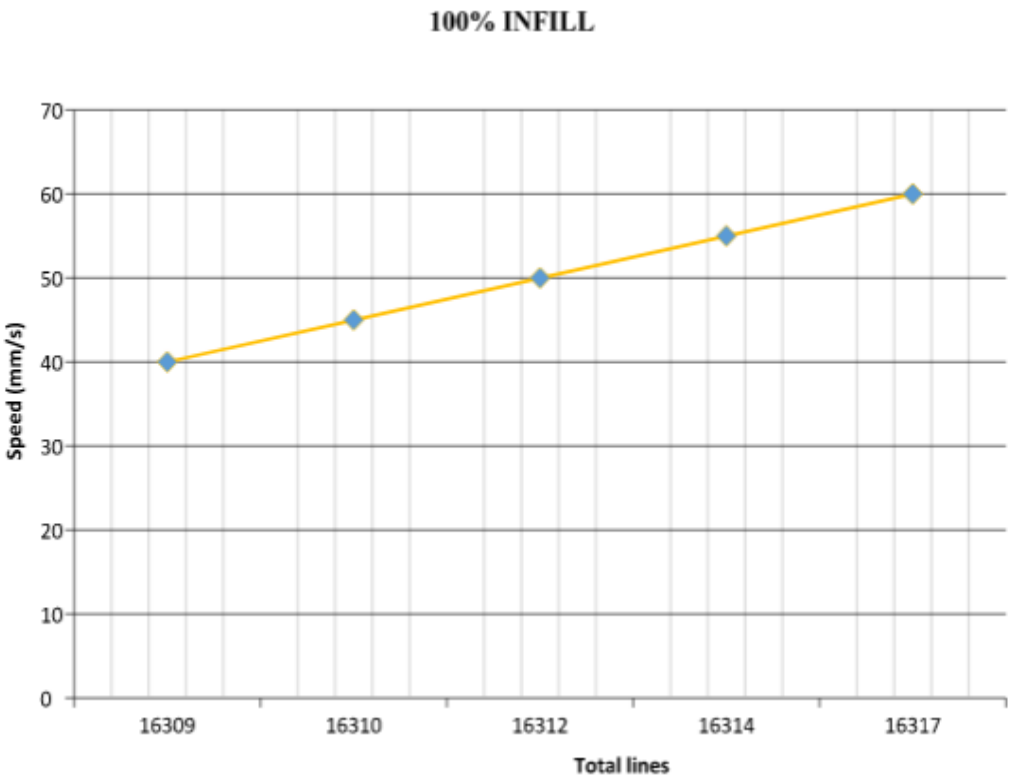

Figure 3.9: Graph of printing speed against total lines of printing for quarter balls at 100% infill

In conclusion, results obtained from Tables 3.1 to 3.6 and represented graphically in Figures 3.1 to 3.6 gives an inversely proportional relationship between printing speed and time of printing of the half balls. The graphs as depicted in Figures 3.1 to 3.6 are linear in nature and its slope gives acceleration of the printing nozzle of the 3D printer. Also, Table 3.7 and Figure 3.7 represent the relationship between each infill percentage and total time of printing of the half balls. A directly proportional relationship is observed between the different infill percentages and their respective total time of printing. This implies that to save materials and ensure a less time for the printing of the models, an infill of 0% is preferable. However, to obtain an excellent quality of printing, an infill of 100% is the best option. Tables 3.8 to 3.9 and Figures 3.8 to 3.9 shows a directly proportional relationship between printing speed and total lines of printing for quarter balls at 0% and 100% infill respectively.

IV. SUMMARY

The creation of models of Body Centered Cubic (BCC) and Face Centered Cubic, (FCC) crystallographic lattice structures for instructional purposes of Atomic Packing Factor, (APF) is aimed at enhancing students understanding of the concept of crystallography. Material properties considered for the creation of these models are aesthetics, strength, transparency and ease of processing. The model is first designed using AutoCAD software. The AutoCAD design of the model is then converted to Standard Tessellation Language (STL) to ensure there are no overlaps in the design. The converted model is made to pass through the process called slicing which converts the Auto CAD drawing into a form in which the 3D printer can understand. The 3D printer then prints the models based on instructions in form of generic codes (G codes) which tells the 3D printer the axes, shape, thickness, speed etc. of printing to be done. At the completion of the printing process, the models are assembled into Body Centered Cubic (BCC) and Face Centered Cubic (FCC) Crystallographic Lattice Structures by the aid of adhesive glue and packaged in transparent boxes made of acrylic. A simplified approach to the computation of Atomic Packing Factor (APF) as presented in this research work showed that the APF of BCC and FCC has a numerical value of 0.68 and 0.74 respectively. Results obtained from the printing of the models showed that there exists an inverse proportional relationship between time of printing and speed of printing. A direct proportional relationship is observed between total

time of printing and each infill percentage, printing speed and total lines of printing for the half and quarter balls respectively. These models having been created will enable the students to have a better optical appreciation of these structures with respect to their Atomic Packing Factor (APF) computation, enhance students understanding of the concept of crystallography and rekindle the interest of the study of crystallography amongst students of material science, crystal chemistry and metallurgy.

REFERENCES

[1]. Adikwanduaba, S. (2005). Technology of Properties of Engineering Materials, Gabtony & Associate Nigeria limited, 133/135 Weatheral Road, Owerri. Pp: 54-128.

[2]. Jorge, A., Luis, D., Javier, M., Carlos, A. and Sergio, C. (2015). An Immersive 3D Visual LearningEnvironment for Analyzing the Atomic Structure of MEMS. Relevant materials, Procedia Computer Science, Volume 75, pp:413-416.

[3]. Krause, S (2012), "Uncovering and Repairing Crystal Structure Misconceptions in an Introductory Materials Engineering Class".

[4]. Stephen, K. Chris, D. Justin, N. Terry, A., and Richard, G. (2002). Identifying Student Misconceptions in Introductory Materials Engineering Classes, Department of Chemical and Materials Engineering, Arizona State University.